Research Article

Received: 29 April 2014 Revised: 1 July 2014 Accepted article published: 8 July 2014 Published online in Wiley Online Library:

(wileyonlinelibrary.com) DOI 10.1002/jctb.4475

Modified chitosan as an economical support for hematin: application in the decolorization of anthraquinone and azo dyes

Agostina Córdoba,[a*] Ivana Magario[a] and María Luján Ferreira[b]

Abstract

BACKGROUND: Azo and anthraquinone dyes have been successfully decolorized using enzymatic and biomimetic homogeneous systems.[1,2] Hematin, a horseradish peroxidase (HRP) biomimetic, immobilized on chitosan via glutaraldehyde coupling was able to decolorize Alizarin Red S and Orange II solutions. A Doehlert experimental design and response surface analysis was applied to determine conditions for optimal mass of catalyst and catalytic efficiency of the immobilization procedure.

RESULTS: The catalysts with supported hematin showed 33% activity (relative to homogeneous hematin as 100%) in decolorization reactions. After six reuses the catalytic activity was maintained at 60% of the initial one. Hematin anchoring to chitosan without alteration of the iron-porphyrin ring was confirmed by ICP, FTIR and UV/visible spectrophotometric methods. In addition, the effect on hematin activity in the decolorization of aminopropyltriethoxysilane (APTS) as a 'spacer arm' between hematin–glutaraldehyde and chitosan was studied.

CONCLUSIONS: An economical heterogeneous catalyst alternative to HRP has been obtained. The spacer arm improves the catalyst´s performance with activities as high as 57% relative to homogeneous hematin. These results support the notion that the activity loss of supported hematin is caused by the restricted access to Fe of the bulky phenolic dyes.

Keywords: supported hematin; peroxidase; chitosan; Alizarin Red S; Acid Orange II

NOTATION

C-GA-Hematin: chitosan-glutaraldehyde-hematin
C-GA-HRP: chitosan-glutaraldehyde-horseradish peroxidase
C-APTS-GA-Hematin: chitosan-aminopropyltriethoxysilane-glutaraldehyde-hematin

INTRODUCTION

Textile industries consume huge amounts of water (almost 100 L per 1 kg of textile material processed), and the water released during the dying process corresponds to 65% of total wastewater.[3,4] About 15% of the total dyes used in these industries are discharged in the effluents. The composition of textile wastewaters varies depending on the particular textile industry. However, they are characterized by high chemical and biological oxygen demands, alkaline pH-values and by strong colorization.[5] Due to the complex structures and synthetic origin of dyes, textile effluents are very difficult to treat using conventional processes.[4–7] Azo and anthraquinone dyes represent two main groups of extensively used dyes.[6]

Enzymatic decoloration has been widely studied. Peroxidases can catalyze these reactions. During their catalytic cycle they form a π-cation radical (Compound I). This active intermediary may react with phenolic substrates to form a radical which can polymerize or degrade.[8,9] Decolorization of anthraquinone (Alizarin Red) and triphenylmethane dyes (Crystal Violet) using chloroperoxidase (CPO), was analyzed in the work of Liu *et al.*[7] The removal of Alizarin Red reached 98%, in only 7 min at mild CPO concentration, but the optimal pH operating value was 3. Remazol Brilliant Blue R was decolorized by a peroxidase from *Aspergillys oryzae* supported in silica-based foam. The maximum activity (83%) was reached at pH 5.[10] In a recent study, Acid Black 1 and Reactive Blue 19 removal using horseradish peroxidase (HRP) was studied. Dye removal

* *Correspondence to: Agostina Córdoba, Investigación y Desarrollo en Tecnología Química (IDTQ), Grupo Vinculado PLAPIQUI - CONICET. Facultad de Ciencias Exactas, Físicas y Naturales, Universidad Nacional de Córdoba, Av. Vélez Sarsfield 1611, X5016GCA, Ciudad Universitaria, Córdoba, Argentina. E-mail: agostinacordoba@gmail.com*

a *Investigación y Desarrollo en Tecnología Química (IDTQ), Grupo Vinculado PLAPIQUI - CONICET. Facultad de Ciencias Exactas, Físicas y Naturales, Universidad Nacional de Córdoba, Av. Vélez Sarsfield 1611, X5016GCA, Ciudad Universitaria, Córdoba, Argentina*

b *Planta Piloto de Ingeniería Química (PLAPIQUI), PLAPIQUI-UNS-CONICET, Universidad Nacional del Sur, Camino La Carrindanga Km 7, CC 717, 8000, Bahía Blanca, Provincia de Buenos Aires, Argentina*

was high (70%) and the level of decolorization was maintained after three reuses.[11] The immobilization of HRP in titania particles improves the stability of the enzyme related to pH variation. The optimum pH was 5 for the soluble HRP and 7 for the immobilized HRP. After five repetitive uses, dye removal decreased to near half of the initial removal efficiency. This declination in removal efficiency can be attributed to the mass transfer limitations due to adsorption of oligomerization products onto immobilized HRP.[12]

The advantages of biomimetic systems include: (1) lower cost; (2) higher stability; (3) the possibility of multiple reuses without inhibition; and (4) lower selectivity due to the absence of proteic structure. A new heterogeneous biomimetic system based on carbon-fiber supported hemin was described by Yao *et al.*[13] The catalytic oxidation of azo dye (RR195) was used as the model molecule. The RR195 removal was stable from pH 1.16 to 9.25 using the supported hemin, whereas in the soluble form hematin only was active at very acidic pH. New reactions may be envisaged when O_2 is present, to generate superoxide and several other intermediates.[14] Our group has studied the immobilization of HRP and hematin in magnetite but there were several practical problems with the catalysts.[15] A preliminary study on the comparison of hematin and HRP was carried out but the biomimetic catalyst needed to be optimized.[16] Azo and anthraquinone dyes have been successfully decolorized by enzymatic and biomimetic homogeneous systems at alkaline pH by our group.[1,2] Aspects of hematin reaction mechanism have been discussed in these works. In addition, kinetic modelling results confirm the presence of the same HRP catalytic intermediaries (unpublished results). According to these results, we postulate that dye molecules interact with activated hematin (like Compound I), and an organic dye radical is formed by hydrogen abstraction from the dye by the Compound I of hematin. Radical attack and reordering are responsible for further degradations.

The recent literature on the topic emphasizes: (1) the problems found with immobilized enzymes in terms of stability and inhibition; (2) the suitability of biomimetic as a cheaper but very active alternative to enzymes, with the ability to be reused several times without inhibition as in the case of HRP; (3) the need for systematization in the preparation of biomimetic catalysts. In this sense, hemin and hematin are highly attractive as metalloporphyrins, even when the use of hematin is hindered due to the low solubility of hematin in acidic media. The heterogeneization of hematin is a solution to this problem, and the use of experimental design methodology is a very powerful tool to obtain optimal parameters for catalyst preparation.

Table 2. Reactions conditions employed in activity measurements

	Hematin		HRP	
	OII	ARS	OII	ARS
[Catalyst] (mg L^{-1})	12	10.5	8.1	6.6
[H_2O_2] (mmol L^{-1})	2.7	6.6	1.36	6.6
pH	10.6	9	10	9

Chitosan is a linear polysaccharide produced by alkaline deacetylation of chitin.[17] Different chitosan modifications can be undertaken to enhance its properties as a catalyst support. Its use as an enzyme support has been widespread in recent years due to low cost, resistance to attrition and biodegradability. In a previous exploratory work, it was found that chitosan could be a suitable support for HRP and hematin, especially for Alizarin removal.[12] Based on that preliminary work, the goal of this work is the evaluation of a supported catalyst based on hematin able to mediate in the decolorization of anthraquinone and azo dyes as a horseradish peroxidase mimetic. Orange II (OII) and Alizarin Red S (ARS) were selected as model dyes. Glutaraldehyde-modified chitosan is proposed as an economical alternative for hematin immobilization. FTIR and ICP characterization of the immobilized hematin, UV-Visible analyses of the glutaraldehyde–hematin coupling reaction, decolorization activity measurements, and HRP as a comparison catalyst are presented and discussed. In addition, the effect of aminopropyltriethoxysilane (APTS) as a 'spacer arm' between hematin–glutaraldehyde and chitosan in the catalyst activity is presented in this study.

MATERIALS AND METHODS

Materials

Hematin ($M_w = 633.49$) from Sigma Co. (USA) and horseradish peroxidase (HRP) from Amano Inc. (Elgin, USA) were used as provided. Chitosan from Primex (Siglufjordur, Iceland) was used as supplied by the provider. Glutaraldehyde 25% (GA) ($M_w = 100.12$) and (3-Aminopropyl)triethoxysilane ($M_w = 221.37$) were supplied

Table 1. Doehlert array of the two variables in experiments

	Factors		Responses				
Exp. N°	[Glutaraldehyde] (mmol g^{-1})	[Hematin] (mmol g^{-1})	Supported Hematin (mmol g^{-1})	Catalyst activity -OII- (μmol $_{OII}$ (g h)$^{-1}$)	Catalyst activity -ARS-(μmol $_{ARS}$ (g h)$^{-1}$)	Intrinsic activity -OII-(μmol$_{OII}$ ($mg_{Hematin}$ h)$^{-1}$)	Intrinsic activity -ARS- (μmol$_{ARS}$ ($mg_{Hematin}$ h)$^{-1}$)
1*	2.50	0.095	$0.063_{(\pm 0.009)}$	$105.1_{(\pm 21.5)}$	$128.7_{(\pm 45.1)}$	$18.1_{(\pm 2.8)}$	$22.1_{(\pm 6.5)}$
2	2.50	0.189	0.094	104.1	117.2	10.8	12.2
3	4.66	0.142	0.070	99.1	127.8	15.5	19.9
4	4.66	0.047	0.044	102.9	90.1	23.2	20.4
5	2.50	0.000	-	34.3**	5.7**	-	-
6	0.33	0.047	0.044	44.2	72.4	14.4	23.6
7	0.33	0.142	0.118	138.0	170.9	14.1	17.5

*Central point.
**Corresponding to modified chitosan absorbance measurements.

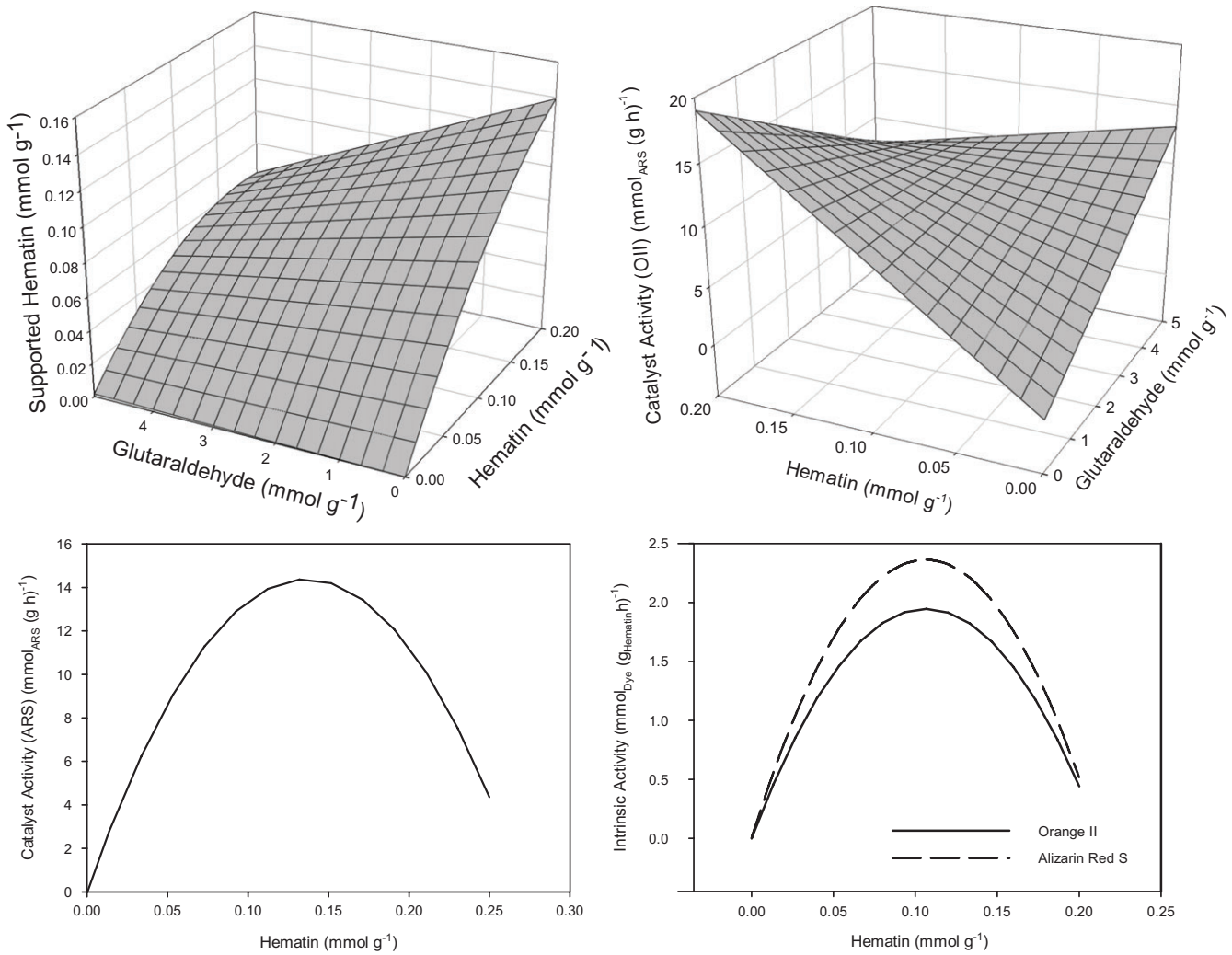

Figure 1. Response surface. Plots of final equations obtained by fitting experimental responses of Table 1 to quadratic models.

by Sigma Aldrich (USA). Alizarin Red S (C.I.:58005) was supplied from Farmitalia Carlo Erba, Montedison Group (Milano, Italy) and Orange II (C.I.:15510) by Merck KGaA (Darmstadt, Germany). All salts were of analytic grade. Solutions were prepared with bidistilled water. Hydrogen peroxide 30 %vol. (2.68 mmol L^{-1}) was provided by Apotarg Laboratories (Córdoba, Argentina).

Table 3. Determination of total iron content of supported catalyst by inductively coupled plasma atomic emission spectroscopy vs. UV-visible

	ICP	UV-visible
Fe (mg $g_{wet\ catalyst}^{-1}$)	$0.591_{(\pm 0.070)}$	$0.508_{(\pm 0.040)}$
Hematin (mmol $g_{wet\ catalyst}^{-1}$)	$0.011_{(\pm 0.001)}$	$0.009_{(\pm 0.001)}$

Characterization techniques and equipment

A Perkin-Elmer Lambda 35 spectrophotometer (Massachusetts, USA) was used for all the UV/Visible measurements. A JASCO FT/IR 5300 instrument (4 cm^{-1} resolution) equipped with a DTGS detector was used for the FTIR studies. Solid samples were dried in an oven at 60 °C overnight. Then, they were ground with KBr powder at 1% wt/wt and pressed to form a thin disk. The reference was air.

Total iron content determinations on the supported hematin preparations were carried out by atomic emission spectrometry–inductively coupled plasma (ICP-AES). For these measurements wet particles were submitted to acid attack (with previously ultra-purified nitric acid) at high temperature using a MARS-5 microwave digester (CEM Corporation, USA) according to standard US EPA method SW-3052. A simultaneous ICPE-9000 high resolution inductively coupled plasma–atomic emission spectrophotometer (Shimadzu, Japan) was used.

Hematin immobilization: experimental design

In order to evaluate the best immobilization conditions, an experimental design based on the response surface methodology was employed. This tool allows the inclusion of the interaction effects among independent variables. Doehlert arrays have the particularity of being more uniform, it having an equally spaced point's distribution. In contrast to familiar designs, Doehlert arrays are more efficient (number of experiments $k^2 + k + 1$ with k the number of factors-independent variables).[18] A Doehlert experimental array with two factors was applied to determine the optimal mass of GA and Hematin for 1 g of chitosan. The factors studied were GA and

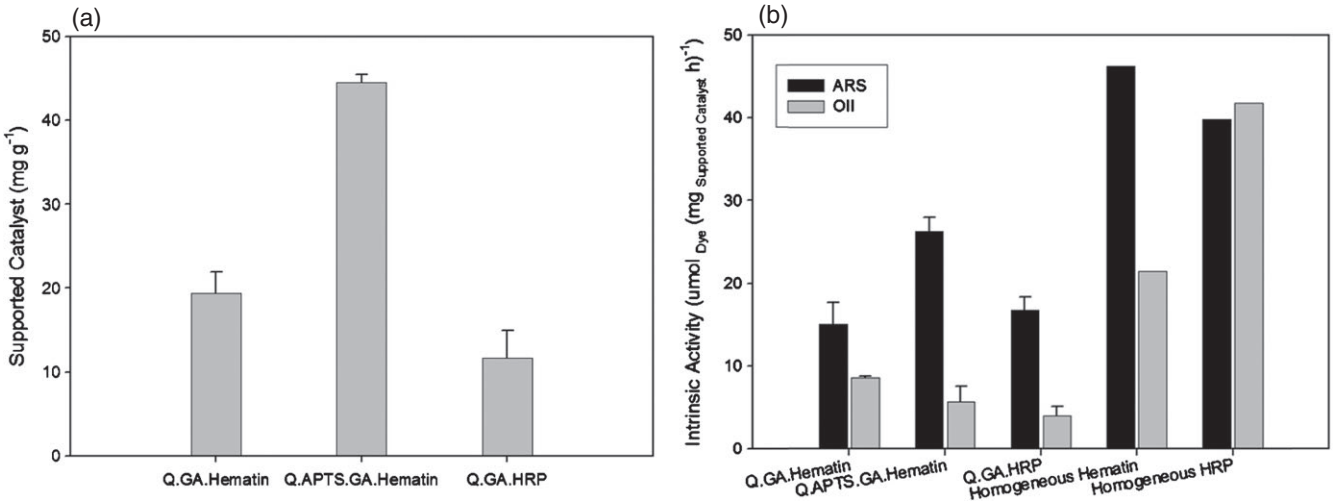

Figure 2. (a) Supported catalyst. Immobilization conditions were: 85 mg g^{-1} hematin to chitosan mass ratio and 0.87 mmol g^{-1} GA to chitosan mass ratio for Q-GA-Hematin and Q-APTS-GA-Hematin; 60 mg g^{-1} HRP and 0.33 mmol g^{-1} GA to chitosan mass ratio for Q-GA-HRP and 3.435 mmol g^{-1} APTS to chitosan mass ratio for Q-APTS-GA-Hematin. (b) Catalyst activity. Homogeneous and heterogeneous intrinsic activity of hematin and HRP.

Hematin expressed in mmol $g_{chitosan}^{-1}$. The measured responses were: supported hematin (mmol $g_{catalyst}^{-1}$), catalytic activity in OII and ARS decolorization (μmol_{dye} $(g_{catalyst}\ h)^{-1}$) and intrinsic activity in OII and ARS decolorization (μmol_{dye} $(mg_{Hematin}\ h)^{-1}$). The experimental matrix is presented in Table 1 with the responses obtained. Experimental responses were fitted to multivariate polynomial models. Statgraphics Centurion XV.2 (Virginia, USA) was used to perform the statistical analysis of the experimental data. Polynomial models that fit the responses studied were obtained by multiple regressions until a satisfactory goodness of fit (good R^2 values) was obtained. To evaluate the statistical significance of the complete set of factors and their interactions an ANOVA test was used. The resulting non-statistical factors were suppressed. The model hierarchy was always maintained.[19] To obtain the optimal balance between factors studied the desirability function (DF) was included to maximize the responses.[20,21]

The heterogeneous catalyst preparation process includes the following steps: (1) chitosan surface activation with GA to produce —C═O groups; (2) immobilization procedure in which hematin or HRP was fixed onto chitosan; (3) —C═O free groups deactivation with a Tris concentrated solution. Analysis of the responses implies unreacted hematin determination and activity measurements in OII and ARS decolorization reactions. All concentrations were expressed per gram of support.

Chitosan surface modification

In order to characterize the chitosan the amino surface density was determined using the Bartkowiak *et al.* method,[22] with OII adsorption under alkaline conditions. The $-NH_2$ surface density in chitosan was 7.3% wt/wt. The GA:NH_2 molar ratios used for the Doehlert design was varied from 0.56 to 1.05. Chitosan surface activation was carried out in 15 mL falcon tubes. Then, 0.1 g of chitosan was added into 5 mL of buffer phosphate pH 7 with the corresponding volume of GA 25% wt/wt commercial solution (from 0.013 mL to 0.176 mL in each experiment – see Table 1). The reaction time was 1 h with magnetic stirring at room temperature (25 °C). After that, the solutions were centrifuged (10 min at 3600 rpm) and washed three times with 10 mL of buffer pH 7.

Immobilization procedure

The wet particles obtained in the surface activation step were added into the corresponding volume of hematin solution (1054.3 mg L^{-1}, in NaOH 0.01 N) (from 0 mL to 11.4 mL – see Table 1) with magnetic stirring at room temperature. After 2 h, the solutions were centrifuged (10 min at 3600 rpm) and washed three times with 10 mL of bidistilled water. Supernatant samples were withdrawn and absorbance at 387 nm was measured for determination of supported hematin by mass balance ($\epsilon = 0.082437$ L mg^{-1}).

Finally, glutaraldehyde -C═O free group deactivation was carried out by the reaction of wet particles with 5 mL of 0.5 mol L^{-1} tris solution with magnetic stirring at room temperature. After 1 h, the solutions were centrifuged (10 min at 3600 rpm) and washed three times with 10 mL of bidistilled water. Supernatant samples were withdrawn and absorbance at 387 nm was measured to determine the unreacted hematin mass.

HRP immobilization

To obtain a reference for hematin, HRP immobilization was carried out. The chitosan surface activation and catalyst immobilization were performed as described above for hematin with 0.33 mmol g^{-1} of GA and 60 mg g^{-1} of HRP. Evaluated responses were the same as for supported hematin.

Activity measurements

Optimal decolorization conditions for each dye were evaluated in previous work[1,2] and maintained in the present study. Reaction conditions are detailed in Table 2. A 200 mg L^{-1} OII or ARS solution was contacted with the wet mass equivalent of heterogeneous catalyst corresponding to each case. Reaction started when H_2O_2 was added. Reaction was carried out in 10 mL of corresponding buffer. After 1 h solutions were centrifuged (10 min at 3600 rpm) and samples withdrawn. Absorbance measurements at selected wavelengths (484 nm for OII and 511 nm for ARS) were used to determine dye conversions.

ARS was used as a phenolic substrate to study the catalyst reuses. Activity after 1 h reuse was carried out as described above for ARS. Also, conversions obtained for 24 h of reaction were evaluated up to the sixth use.

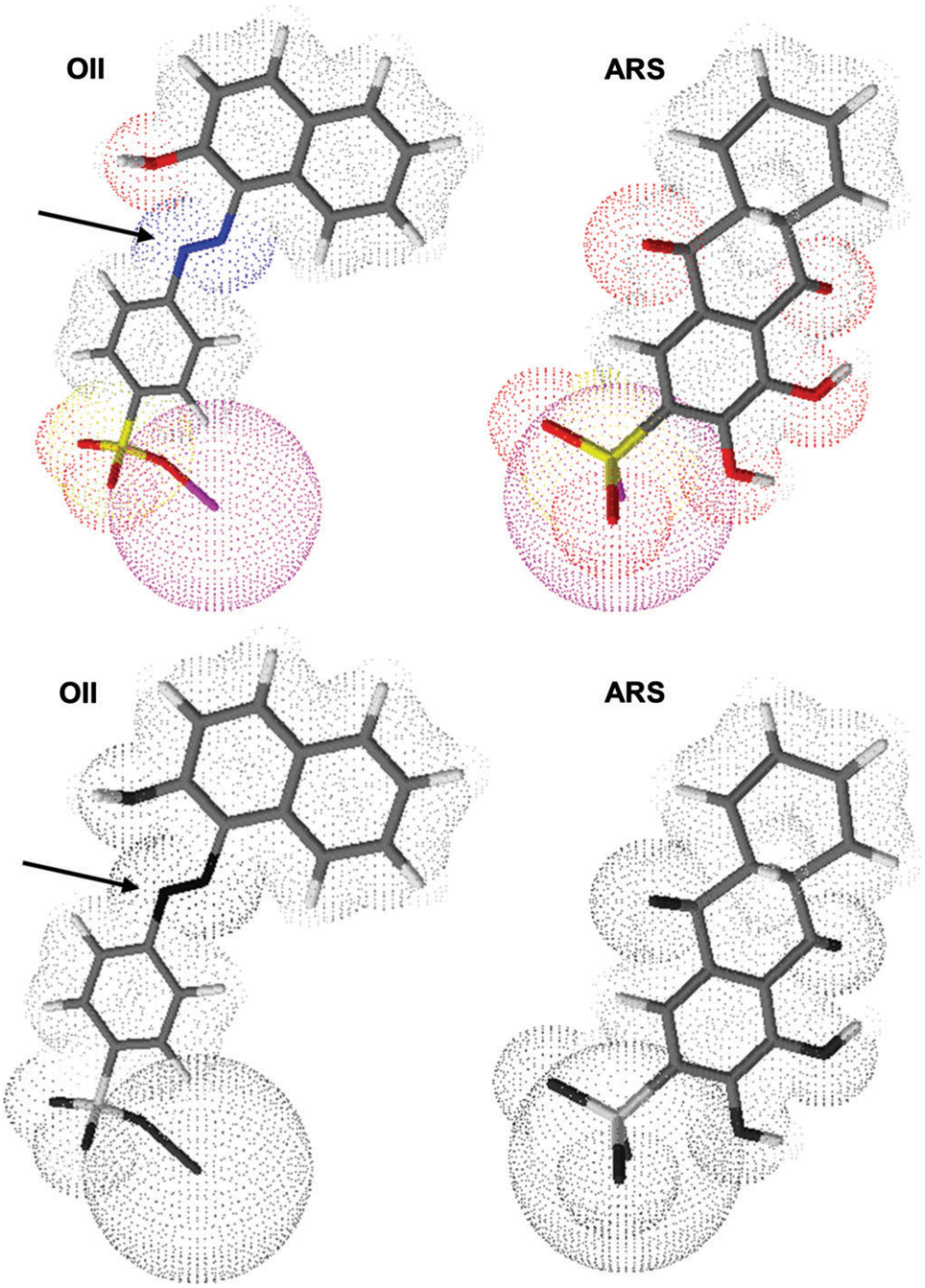

Figure 3. Dye structure. ARS and OII structures. The arrow shows the rotation point of the molecule.

Catalysts characterization

In order to study the hematin:GA interaction in solution, UV-Visible absorbance measurements during reaction were carried out. Reaction was performed in a quartz cuvette at 0.29 mmol L^{-1} GA and 0.0029 mmol L^{-1} hematin aqueous solution. FTIR spectra of hematin, chitosan, chitosan activated with GA, supported hematin and supported HRP were recorded in the 4600–400 cm^{-1} range. The solids obtained from the central points of the Doehlert design (experiment N°1, Table 1) were analyzed for total iron content using atomic emission spectrometry for inductively coupled plasma (ICP-AES).

APTS as 'spacer arm'

In order to evaluate the effect of the separation between hematin and chitosan surface, APTS was used as a 'spacer arm'. A 0.1 g sample of chitosan was contacted with 77.6 µL of 98% APTS in 5 mL of phosphate buffer pH 7 with magnetic stirring at room temperature. After 2 h, solutions were centrifuged (10 min at 3600 rpm) and washed three times with 10 mL of bidistilled water. After that, chitosan surface activation and catalyst immobilization were performed as described previously (GA:0.87 mmol g^{-1}; Hematin 0.134 mmol g^{-1}). Supported hematin and catalytic and intrinsic activity were evaluated for both dyes. The catalyst obtained was also characterized as described in the previous section.

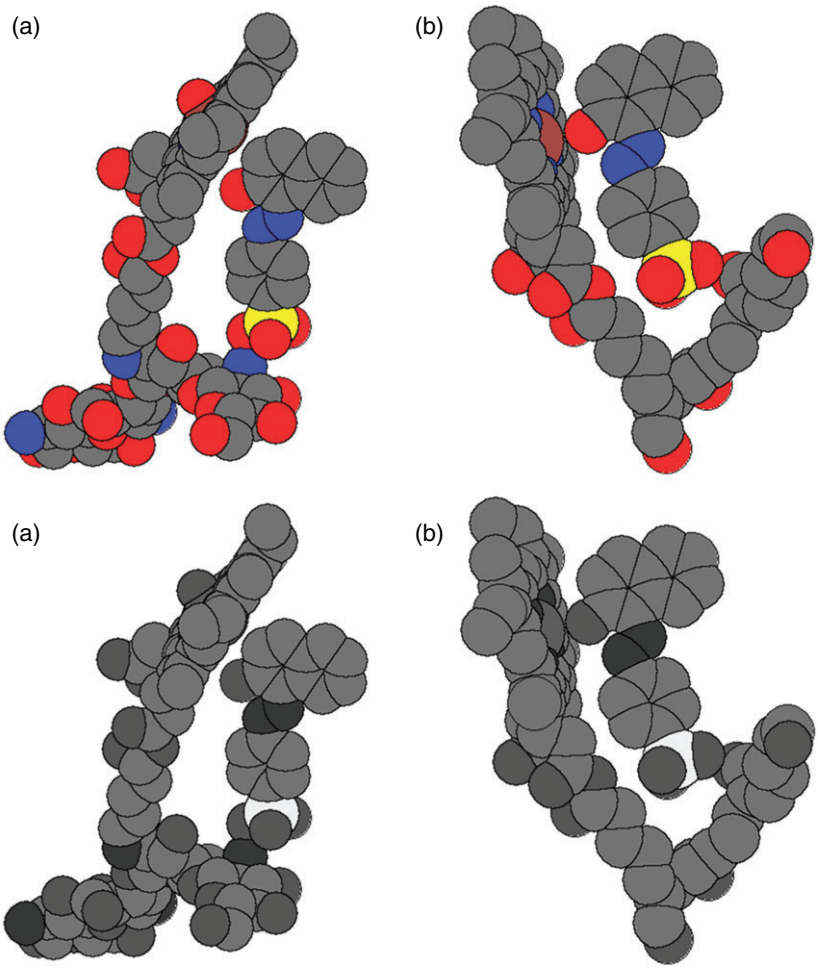

Figure 4. Steric hindrance when Orange II is adsorbed onto chitosan, near hematin linked through monomeric glutaraldehyde. (a) Interaction among Orange II, Hematin (linked by monomeric glut to chitosan) and Chitosan. (b) Interaction among Orange II, Hematin and Polyglut.

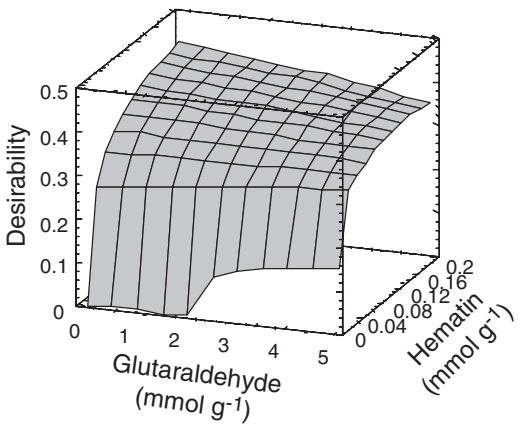

Figure 5. Optimization. Desirability function considering supported hematin, catalytic activity and intrinsic activity with OII and ARS.

RESULTS AND DISCUSSION

Hematin immobilization

The response surfaces obtained by fitting experimental data to quadratic models are shown in Fig. 1. Hematin was unable to be immobilized using low hematin concentrations. On the other hand, at high hematin concentration, the best results were obtained with surface modification under low GA concentration conditions. This result can be attributed to the existence of GA oligomers on the chitosan surface from GA solutions, which hinder the proper hematin–GA interaction.[23,24] The amount of supported hematin determined by UV/visible measurements of hematin remaining in supernatants was supported by total iron content analysis in solid catalysts using ICP. Results are presented in Table 3. The agreement of both determinations confirms hematin immobilization. In addition, the presence of iron in the particles confirms no metal leaching during the immobilization process.

The activity measurements for OII and ARS decolorization further confirmed hematin immobilization on chitosan surface. The catalytic activity in OII removal was in line with the results of supported hematin. With ARS as substrate, GA concentration did not have a statistically significant effect on catalytic activity. This response was maximum at medium values of hematin loading. A high hematin input was required to obtain immobilization yields of 95% of supported hematin, but the activity of supported hematin (called intrinsic) with both substrates was highest at 0.1 $mmol_{Hematin}$ $(g\,h)^{-1}$ decreasing thereafter. The existence of a maximum for the intrinsic activity at 0.1 $mmol_{Hematin}$ $(g\,h)^{-1}$ can be assigned to: (1) catalyst modification by formation of covalent bonds with modified chitosan; (2) metalloporphyrin aggregation on the chitosan surface [25,26] or hematin dimers formation; or (3)

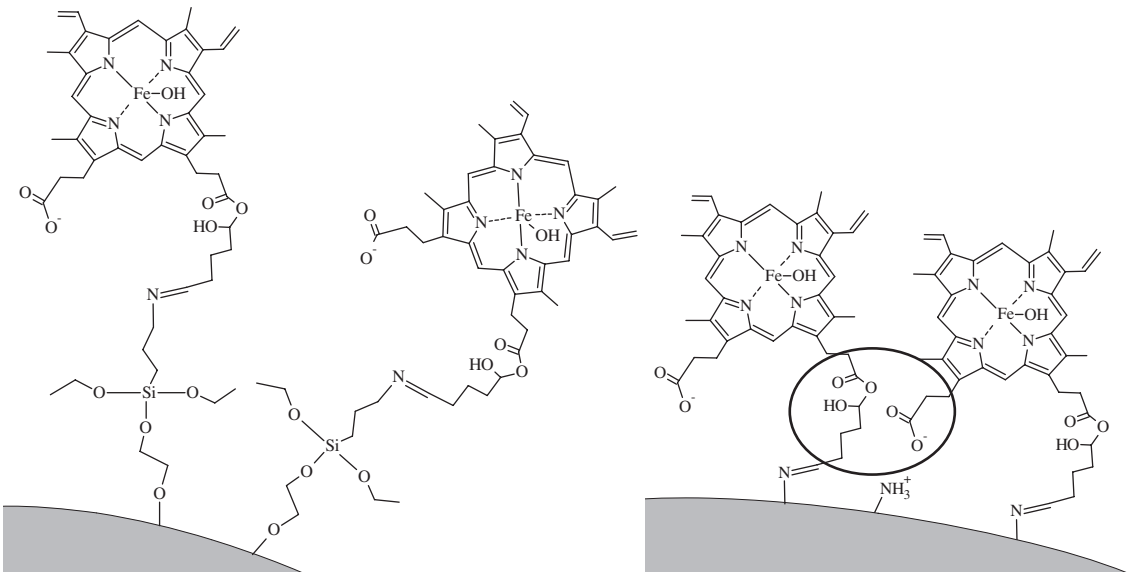

Figure 6. APTS as 'spacer arm'. Effect of the 'spacer arm' on hematin immobilization.

restricted access of the substrate to the Fe catalytic site of hematin. Considering the independence of the intrinsic activity from GA input, the first option (1) was discarded. Thus, we can propose that the interactions between the coupling agent and hematin do not produce deactivation.

The intrinsic activity of homogeneous and heterogeneous catalysts is presented in Fig. 2. The decrease in activity of immobilized hematin vs. free hematin was observed not only for OII, but also for ARS. With ARS as substrate, intrinsic activity decreased from 46 (homogeneous biocatalyst) to 15 μmol_{ARS} $(mg_{Hematin}\ h)^{-1}$ (for Q-GA-Hem). For the same catalyst and azoic substrate decolorization the intrinsic activity decreased from 21.5 to 8.6 μmol_{OII} $(mg_{Hematin}\ h)^{-1}$. The observed difference can be attributed to the nature of the substrate. ARS has a plane structure while OII has a single bond that permits its rotation (see Figs 3 and 4), and access to the sixth coordination position of Fe in hematin may be difficult.

This can result in major local H_2O_2 concentration in the vicinity of the catalytic site. The relative increase in H_2O_2 to phenolic substrate concentration can generate two main routes of reaction: the porphyrin inactivation by reactions with excess of H_2O_2 ,[27,28] or a catalatic-like pathway with O_2 formation.[1,2] In previous studies of ARS decolorization, we observed the release of O_2 during hematin homogeneous catalysis.[1] Also, hematin is a catalase biomimetic, too.

Figure 2 shows the interaction between hematin onto chitosan and OII. The dyes may be close to the chitosan surface and be adsorbed. ARS and OII are adsorbed strongly on chitosan,[29] in such a way that the blocking of one side of hematin could be assigned to the location of the adsorbed dye, near the iron. It is known that glutaraldehyde is not monomeric, but oligomeric (Polyglut), at least partially. Even in this case, the interaction hematin–dye may produce blocking of the coordination side of the hematin, as Fig. 4(b) shows.

The desirability function was included to determine immobilization conditions for an optimal balance between mass and decolorization efficiencies towards both dyes. This optimal mass proportion was found when 1 g of dried chitosan is activated with 0.33 mmoles of GA and incubated afterwards with 0.19 mmoles of hematin (Fig. 5).

HRP immobilization

In order to evaluate hematin as a potential alternative to HRP, the performance of supported HRP was also considered in this study. The responses obtained are presented in Fig. 2. The OII decolorization was similar to those found due to dye physical adsorption onto chitosan (see Table 1 – experiment N° 5). Nevertheless, with ARS as substrate the intrinsic activity decreased 58% compared with the homogeneous. These results show that by anchoring the catalyst there is a restricted access of the OII substrate to the active site. That produces the activity loss observed. In previous studies,[1,2] we analyzed this interaction and concluded that, in the case of ARS, a water molecule must be present in HRP for compound II formation. A water molecule can act as a bridge between HRP and ARS (involving their two —OH groups) and allow oxidation of the substrate. However, restricted access to the active site due to the immobilization and the catalyst inactivation during immobilization results in low conversions. H_2O_2 inactivation can also occur by increasing local peroxide concentration.[30] Besides, the enzyme inactivation by radical attacks increases with immobilization.[31–33] Xialing *et al.* reported that the organic radicals formed remain near the enzyme and promote its inactivation.[34] These radicals may be adsorbed on chitosan near the hematin when APTS is not used.

APTS as spacer arm

APTS was used as a *spacer block* in order to analyze the restricted access of substrates to supported hematin. Measured responses are presented in Fig. 2. As for HRP, intrinsic activity values of C-APTS-GA-Hematin for OII as substrate corresponds to removal by adsorption onto chitosan rather than actual hematin activity (see Table 1 – experiment N°5). Concerning ARS, activity losses were registered during the immobilization process. However, intrinsic activity decreased from 46.2 (homogeneous biocatalyst) to 26.3 $\mu mol_{ARS}\ mg_{Hematin}^{-1}$ (in Q-GA-APTS-Hem). The higher intrinsic activity obtained with APTS as 'spacer arm' can be assigned to steric factors (Figs 6 and 7). Figure 7 shows lateral views of OII near hematin linked to chitosan. It is clear that there was a repulsive interaction when OII was located near the surface, by the side of hematin that includes the 'arm bond' to the chitosan. There is a 50/50 chance

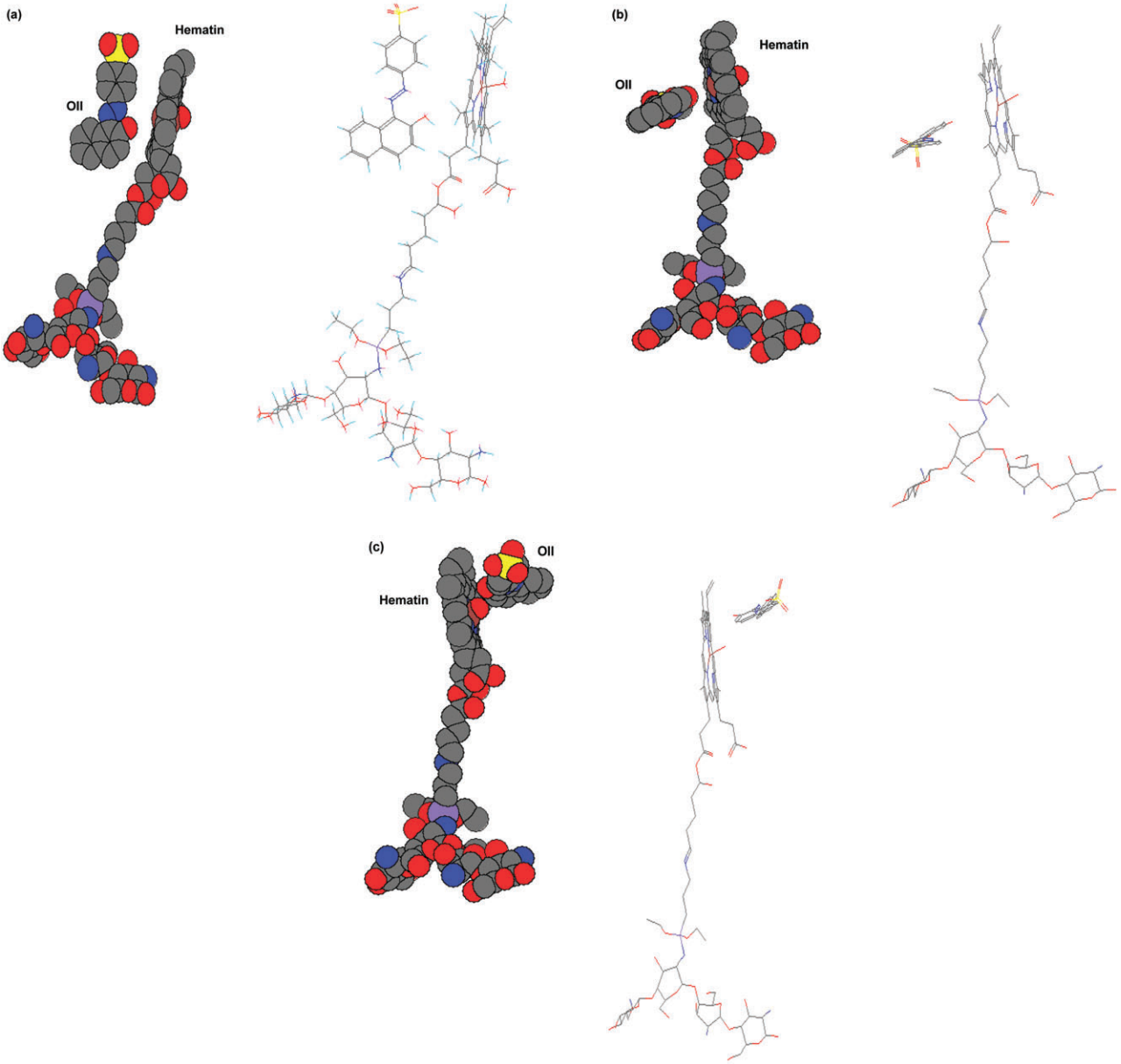

Figure 7. Spatial interaction sustrate-catalyst. (a) Location I of Orange II-inward. (b) Location II of Orange II-inward. (c) Location III of Orange III-outward.

that the -OH stays on the inner or in the outer side of hematin. If the -OH is inward instead of outward of the location of the spacer arm; there are additional important steric hindrances to the OII coordination. In the case of ARS, these restrictions are much lower due to the planar nature of the ARS structure. Strong adsorption of ARS and OII and their organic radicals onto chitosan when APTS is absent is also a pathway to Fe blocking and /or catalyst´s deactivation (Fig. 4).

Table 4. ARS conversions obtained: first use - 1 h reaction - and sixth use - 24 h reaction

	First use conversions 1 h	Sixth use conversions 24 h
C-GA-Hematin	$29.5_{(\pm 5.76)}$	$17.8_{(\pm 3.28)}$
C-APTS-GA-Hematin	$48.7_{(\pm 4.04)}$	$34.1_{(\pm 4.95)}$
C-GA-HRP	$20.0_{(\pm 1.44)}$	$0.9_{(\pm 1.00)}$

Catalysts reuse

Reuse results are presented in Fig. 8 and Table 4. C-APTS-GA-Hematin presented the highest intrinsic activity. A decrease in activity was found for immobilized hematin. Nevertheless, conversions on the sixth use at 24 h reaction with C-APTS-GA-Hematin and with C-GA-Hematin were 70% and 60% of the first use, respectively. On the other hand, immobilized HRP maintained activity only to the fourth use, and was unable to treat the ARS solution after five uses.

FTIR catalyst characterization

FTIR spectra of the catalysts obtained in different immobilization steps are presented in Fig. 9. The spectrum of chitosan presents

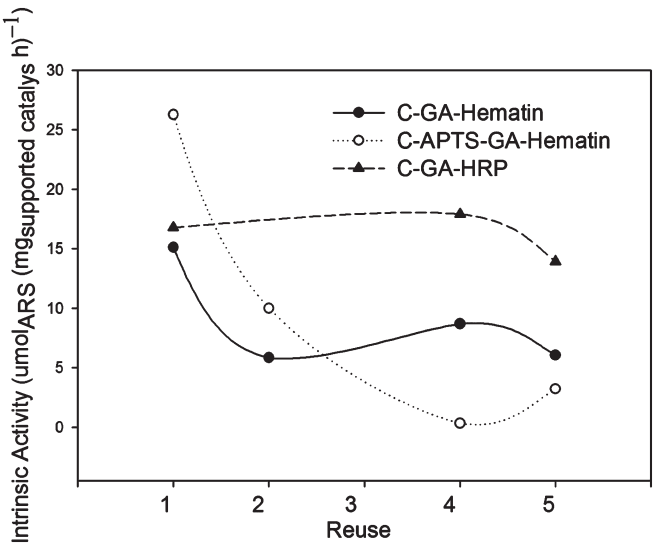

Figure 8. Reuses. Reuse activity of the supported catalyst with ARS as phenolic substrate.

characteristic peaks: at 2962 and 2853 cm^{-1} the vibration peaks of C—H, at 2926 cm^{-1} a band assigned to carbon–hydrogen vibration, and at 895 cm^{-1} the peak corresponding to C—H stress of anomeric groups of chitosan. The presence of —CH_2 was confirmed by the 1421 cm^{-1} absorption band, and —CH and C—CH_3 bond deformation are assignable to the 1378 cm^{-1} band.[35] The peaks at 1036 and 1099 cm^{-1} were assigned to vibrations of chitosan backbone.[17] Peaks between 3600 and 3200 cm^{-1} correspond to O—H and N—H vibrations with strong hydrogen-bonding interactions, and the C—N bond has a signal at 1230 cm^{-1}.[36] Finally, the band at 1154 cm^{-1} is assignable to C—O—C stress vibration.[17] There were slight changes in the FTIR spectra when GA was added, just a growth of the 2878 cm^{-1} peak assignable to symmetric stretching of —CH_2. The peak at 1378 cm^{-1} also grew. The presence of a peak at 1650 cm^{-1} can be associated with C═C from aldol condensation of GA.[23,24] The C═O characteristic peak at 1750 cm^{-1} disappeared.

The spectrum of Q-GA-HRP presents peaks at 1640 and 1650 cm^{-1} corresponding to amide I band region (assignable to primary C═O stretch). Also, the amide II characteristic peaks are present at 1625, 1530 cm^{-1} and 1510 cm^{-1}, which are assignable to N—H band and C—N stretching. This result demonstrates that the secondary structure of the protein was conserved after immobilization.[37–39]

The spectrum of hematin presents peaks at 2920 and 2854 cm^{-1} corresponding to symmetric and asymmetric vibrations of C—H and CH_2. There are also peaks corresponding to symmetric and asymmetric deformation of the H atom of -CH_3 at 1450 and 1380 cm^{-1}. Also noted is the presence of a peak corresponding to the stretching vibrations of the C═C bond at 1625 cm^{-1}. The small peak at 3090 cm^{-1} is associated with the stretching vibrations of═CH_2, while the absorptions between 1000 and 800 cm^{-1} are associated with bending vibrations of═C(H). C—N bonds were confirmed by the peaks at 1360 and 1270 cm^{-1} (doublet product of double bond conjugation). Characteristic bands of the carbonyl group are observed at: 1710 cm^{-1} corresponding to C═O stretching, 920 cm^{-1} assigned to out-of-plane bending C—O—H, and 1240 cm^{-1} to C—O stretching.[41] Also, the peaks for O-H and N-H vibrations are present between 3200 and 3600 cm^{-1}.[42] Peaks at 940, 990 and 1010 cm^{-1} are ascribed to a ring vibration of porphyrin skeleton.[43–45] The band at 1091 cm^{-1} is assigned to pyrrolic C—H.[46] The presence of peaks for O—H and N—H vibrations confirmed that no extensive condensation to produce dimmers took place in the solid.[47] Peaks at 1091 and 1625 cm^{-1} confirmed the presence of porphyrin in supported hematin.

Characterization of hematin–glutaraldehyde linkage

The hematin–GA interaction can be analyzed by means of the observed FTIR signals. Figure 9,c –pointed circles – shows two characteristic ester bands at 1170–1070 cm^{-1} corresponding to —C═O—O—C asymmetric and symmetric stretching, respectively,[40] and bands at 1310–1100 cm^{-1} assignable to C—O—C bonds. Finally, the characteristic bands of the carbonyl group are not present.[40] This is in line with a covalent interaction between the carboxylic acid of hematin and the aldehyde group of GA, instead of a reaction with the —OH of hematin in its fifth coordination position (Fig. 10).

The staked UV-Visible spectra are shown in Fig. 11. The increase in absorbance at 233 nm is assigned to π- > π* transitions due to C═C bond formation because of the aldol condensation of GA.[23,24] A weak band at 285 nm is also observed, assignable to n- > π* transitions of C═O bonds. However, there is no evidence of hematin active site modifications in the UV-Visible study because there are no alterations to the Soret band. The formation of covalent bonds affecting the porphyrinic ring can be discarded. Even more, because of the spatial disposition of hematin, the metalloporphyrin aggregation can also be ruled out.

CONCLUSIONS

A lower cost heterogeneous catalyst alternative to HRP has been obtained. The Doehlert design and desirability functions were used to determine the optimal immobilization conditions at 0.33 mmoles g^{-1} GA and 0.19 mmoles g^{-1} of hematin. Immobilized hematin was able to decolorize ARS solutions after six uses. Catalyst characterization also showed hematin anchoring, and the covalent interaction of carbolylic acid–aldehyde group between hematin and GA. The catalytic site alterations during the inmobilization process have been discarded. That is, neither porphyrin ring modifications by covalent interaction with Q-GA, nor hematin dimmer formations were observed.

Based on the results we can conclude that restricted access of phenolic substrates to the catalytic site and the resulting relative increase in H_2O_2 concentration are responsible for the measured activity loss after immobilization. The use of an APTS 'spacer arm' is a pathway to solve these drawbacks. The higher 'mobility' of the APTS plus glutaraldehyde-linked hematin and the longer distance from the surface allow a 'soluble-like' environment in such a way that the steric hindrance to the coordination of substrate dye molecules is lower.

Strategies to improve catalytic activity and toxicity analysis will be further analyzed in future studies.

ACKNOWLEDGEMENTS

The authors acknowledge the financial support of the Consejo Nacional de Investigaciones Científicas y Tecnológicas (CONICET), Agencia Nacional de Promoción Científica y Tecnológica (ANPCyT, PICT Bicentenario 2010- 0788) and the Universidad Nacional de Córdoba (Argentina). We acknowledge the financial support

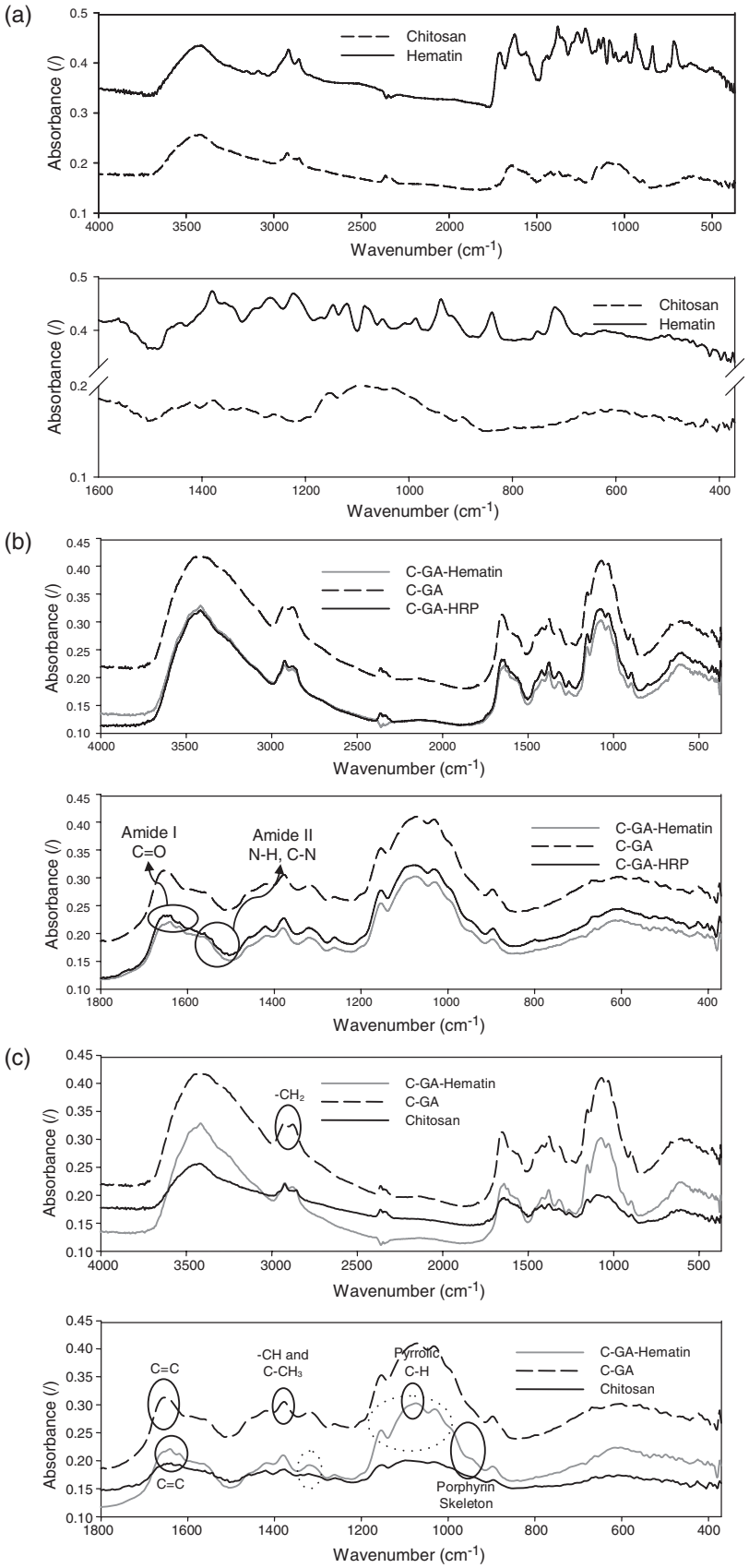

Figure 9. FTIR Spectra. FTIR caracterization of catalysts.

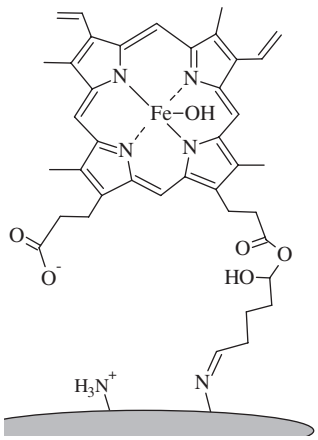

Figure 10. Catalyst structure. Covalent interactions between chitosan —NH_3 groups, glutaraldehyde and hematin.

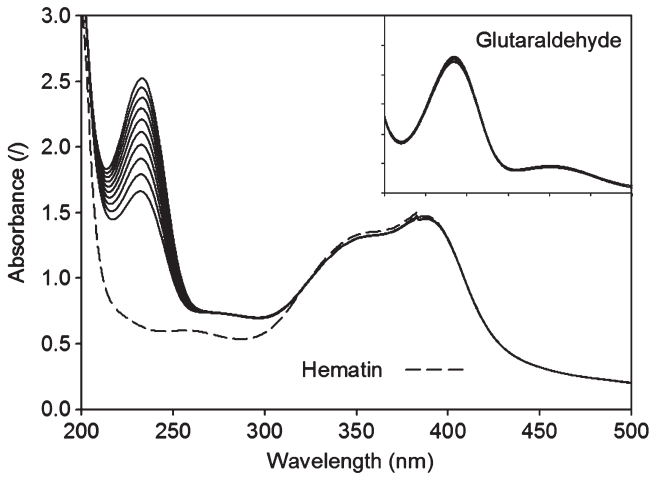

Figure 11. Hematin–Gglutaraldehyde interaction. UV-Visible spectra of the interaction between 0.029 mmol L^{-1} hematin and 29 mmol L^{-1} glutaraldehyde. The inset shows the spectrum of 29 mmol L^{-1} glutaraldehyde in NaOH 0.3 mmol L^{-1} solution (equivalent to hematin solution).

granted through the PRH-03 and the PGI 24/Q022 SECyT-UNS (Bahía Blanca, Argentina). The authors also wish to thank the Departamento de Química Industrial de la Facultad de Ciencias Exactas, Físicas y Naturales de la Universidad Nacional de Córdoba for its collaboration.

REFERENCES

1 Córdoba A, Magario I and Ferreira ML, Experimental design and mm2-pm6 molecular modelling of hematin as a peroxidase-like catalyst in alizarin red s degradation. *J Molec Catal A: Chem* **355**:44–60 (2012).
2 Córdoba A, Magario I and Ferreira ML, Evaluation of hematin catalyzed orange ii degradation as a potential alternative to horseradish peroxidase. *Int Biodeter Biodegrad* **73**:60–72 (2012).
3 Abadulla E, Tzanov T, Costa S, Robra KH, Cavaco-Paulo A and Gubitz GM, Decolorization and detoxification of textile dyes with a laccase from trametes hirsuta. *Appl Environ Microbiol* **66**:3357–3362 (2000).
4 Bandala ER, Tratamiento de agua residual proveniente de la industria textil mediante fotocatálisis solar, XXVIII Congreso Interamericano de Ingeniería Sanitaria y Ambiental, Cancún, México. 27–31 de Octubre (2002).
5 Nigam P, Armour G, Banat IM, Singh D and Marchant R, Physical removal of textile dyes from effluents and solid-state fermentation of dye-adsorbed agricultural residues. *Bioresource Technol* **72**:219–226 (2000).
6 Aspland JR, *Textile Dyeing and Coloration*. American Association of Textile Chemists and Colorists (1997).
7 Liu L, Zhang J, Tan Y, Jiang Y, Hu M, Li S, *et al.*, Rapid decolorization of anthraquinone and triphenylmethane dye using chloroperoxidase: catalytic mechanism, analysis of products and degradation route. *Chem Eng J* **244**:9–18 (2014).
8 Reihmann M and Ritter H, Synthesis of phenol polymers using peroxidases. *Adv Poly Sci* **194**:1–49 (2006).
9 Dunford HB, *Heme Peroxidases*. John Wiley, VCH, USA (1999).
10 Shakeri M and Shoda M, Efficient decolorization of an anthraquinone dye by recombinant dye-decolorizing peroxidase (rdyp) immobilized in silica-based mesocellular foam. *J Mol Catal B: Enzymatic* **62**:277–281 (2010).
11 Celebi M, Arif Kaya M, Altikatoglu M and Yildirim H, Enzymatic decolorization of anthraquinone and diazo dyes using horseradish peroxidase enzyme immobilized onto various polysulfone supports. *Appl Biochem Biotechnol* **171**:716–730 (2013).
12 Jiang Y, Tang W, Gao J, Zhou L and He Y, Immobilization of horseradish peroxidase in phospholipid-templated titania and its applications in phenolic compounds and dye removal. *Enzyme Microbial Technol* **55**:1–6 (2014).
13 Yao Y, Mao Y, Huang Q, Wang L, Huang Z, Lu W, *et al.*, Enhanced decomposition of dyes by hemin-acf with significant improvement in ph tolerance and stability. *J Hazard Mater* **264**:323–331 (2014).
14 Gao Y and Chen J, Redox reaction of hemin-immobilized polyallylamine–polystyrene latex suspensions. *J Electroanalyt Chem* **578**:129–136 (2005).
15 Saidman S, Rueda EH and Ferreira ML, Activity of free peroxidases, hematin, magnetite-supported peroxidases and magnetite-supported hematin in the aniline elimination from water-uv–vis analysis. *Biochem Eng J* **28**:177–186 (2006).
16 Pirillo S, Rueda EH and Ferreira ML, Supported biocatalysts for alizarin and eriochrome blue black r degradation using hydrogen peroxide. *Chem Eng J* **204–206**:65–71 (2012).
17 A.F. Roberts, *Chitin Chemistry*. The MacMillan Press (1992).
18 Doehlert D, Uniform shell design. *Appl Statistics* **19**:231–239 (1970).
19 Gutierrez Pulido H and De la Vara Salazar R, *Análisis y Diseño de Experimentos*, 2nd edn. Interamericana. M-H, editor D.F., Mexico (2008).
20 Ezerra MA, Santelli RE, Oliveira EP, Villar LS and Escaleira LA, Response surface methodology (rsm) as a tool for optimization in analytical chemistry. *Talanta* **76**:965–977 (2008).
21 Murphy TE, Tsui KL and Allen JK, A review of robust design methods for multiple responses. *Res Eng Design* **15**:201–215 (2005).
22 Bartkowiak AW, Roberts GAF, Investigation of sorbates for the determination of the fa values of chitin and chitosan by an adsorption technique. *Polish Chitin Society, Monograph XII* (2007).
23 Migneault I, Dartiguenave C, Bertrand MJ and Waldron KC, Glutaraldehyde: behavior in aqueous solution, reaction with proteins, and application to enzyme crosslinking. *BioTechniques* **37**:790–802 (2004).
24 Shlomo Margel AR, Synthesis and characterization of poly (glutaraldehyde). A potential reagent for protein immobilization and cell separation. *Macromolecules* **13**:19–24 (1980).
25 Bruice TC, Reactions of hydroperoxides with metallotetraphenylporphyrins in aqueous solutions. *Acct Chem Res* **24**:243–249 (1991).
26 Lindsay Smith JR and Lower RJ, The mechanism of the reaction between t-butyl hydroperoxide and 5, 10, 15, 20-tetra(n-methyl-4-pyridyl)porphyrinatoiron(iii) pentachloride in aqueous solution. *J Chem Soc Perkin Trans* **2**:31–39 (1991).
27 Cunningham ID, Danks TN, Hay JN, Hamerton I and Gunathilagan S, Evidence for parallel destructive, and competitive epoxidation and dismutation pathways in metalloporphyrin-catalysed alkene oxidation by hydrogen peroxide. *Tetrahedron* **57**:6847–6853 (2001).
28 Stephenson NA and Bell AT, A study of the mechanism and kinetics of cyclooctene epoxidation catalyzed by iron(iii) tetrakispentafluorophenyl porphyrin. *J Am Chem Soc* **127**:8635–8643 (2005).
29 Pedroni V, Pirillo S, Rueda E and Ferreira ML, Elimination of dyes from aqueous solutions using iron oxides and chitosan as adsorbents. A comparative study. *Quimica Nova* **32**:1239–1244 (2009).
30 Dunford HB, *Heme Peroxidases*. John Wiley, VCH, USA (1999).
31 Nicell JA, Saadi KW and Buchanan ID, Phenol polymerization and precipitation by horseradish peroxidase enzyme and an additive. *Bioresource Technol* **54**:5–16 (1995).

32 Kapeluich YL, Rubtsova MY and Egorov AM, Enhanced chemiluminescence reaction applied to the study of horseradish peroxidase stability in the course of p-Iodophenol oxidation. *J Luminescence* **12**:299–308 (1997).
33 Wagner M and Nicell JA, Detoxification of phenolic solutions with horseradish peroxidase and hydrogen peroxide. *Water Res* **36**:4041–4052 (2002).
34 Cai Xialing ML, Horseradish peroxidase catalyzed free radical cannot free move in reaction solution. *J Biochem Technol* **4**:92–95 (2009).
35 National Standard Reference Data Series, National Bureau of Standards. US Government Printing Office, June 1972. Retrieved 13 December 2012.
36 Conley RT, *Espectroscopia infrarroja*, 1° edicion española. Alhambra, Spain (1979).
37 ElKaoutit M, Naranjo-Rodriguez I, Domínguez M, and J.L. Hidalgo-Hidalgo-de-Cisneros, Bio-functionalization of electro-synthesized polypyrrole surface by heme enzyme using a mixture of Nafion and glutaraldehyde as synergetic immobilization matrix: conformational characterization and electrocatalytic studies. *Appl Surf Sci* **257**:10926–10935 (2011).
38 Monier M, Ayad DM, Wei Y and Sarhan AA, Immobilization of horseradish peroxidase on modified chitosan beads. *Int J Biol Macromol* **46:**324–330 (2010).
39 Xu Q, Mao C, Liu N-N, Zhu J-J and Sheng J, Direct electrochemistry of horseradish peroxidase based on biocompatible carboxymethyl chitosan – gold nanoparticle nanocomposite. *Biosens Bioelectron* **22:**768–773 (2006).
40 Stuart BH, *Infrared Spectroscopy: Fundamentals and Applications*. John Wiley & Sons (2004).
41 Conley RT, *Espectroscopia Infrarroja*, 1° edicion española ed. Alhambra, Spain (1979)
42 Amaravathi M, Babu MM and Chandramouli G, Synthesis of meso-tetrakis (2-chloroquinolin-3-yl) porphyrins. *Arkivoc* 2007:148–153 (**2007**).
43 Parker FS, *Applications of Infrared, Raman, and Resonance Raman Spectroscopy in Biochemistry*, New York (1983).
44 Thomas DW and Martell AE, Visible and ultraviolet absorption spectra of metal chelates of para-substituted tetraphenylporphines. *Archives of Biochemistry and Biophysics.* **76**:286–294 (1958).
45 Huang G, Luo Z-C, Hu Y-D, Guo Y-A, Jiang Y-X and Wei S-J, Preparation and characterization of iron tetra (pentaflurophenyl)-porphyrin (tpfpp fe) supported on boehmite (bm). *Chem Eng J* **195–196**: 165–172 (2012).
46 De Villiers KA, Kaschula CH, Egan TJ and Marques HM, Speciation and structure of ferriprotoporphyrin ix in aqueous solution: spectroscopic and diffusion measurements demonstrate dimerization, but not μ-oxo dimer formation. *J Biol Inorg Chem* **12**:101–117 (2007).
47 Maitra D, Byun J, Andreana PR, Abdulhamid I, Diamond MP, Saed GM, *et al.*, Reaction of hemoglobin with hocl: mechanism of heme destruction and free iron release. *Free Radical Biol Med* **51**:374–386 (2011).

